Recent Charm Physics Results from CLEO

Don H. Fujino[1]

Lawrence Livermore National Laboratory
Livermore, CA 94550
Representing the CLEO Collaboration

Abstract. In this talk I present recent charm physics results from the CLEO experiment. Final state interactions and W-annihilation effects in charmed mesons decays are discussed. These include an isospin analysis of $D \to K\bar{K}$, observation of the candidate W-annihilation decay $D_s^+ \to \omega\pi^+$, and evidence of non-factorizable effects in $D_s^+ \to \eta\pi^+$, $\eta'\pi^+$, $\eta\rho^+$, and $\eta'\rho^+$ decays. Presented next are CLEO's observations of the spin $\frac{3}{2}^+$ excited charmed baryons Σ_c^{*++} and Σ_c^{*0}, and the excited charmed-strange baryons Ξ_c^{*+} and Ξ_c^{*0}. I conclude with future prospects in charm physics with CLEO's new silicon detector.

INTRODUCTION

The external and internal spectator diagrams do an excellent job of explaining most of the features in charmed meson decays. For example, the lifetime hierarchy, *i.e.* the fact that the D^+ meson lifetime is a factor of $2 - 2.5$ times longer than the D^0 or D_s^+ lifetime can be attributed to the destructive interference between the external and internal diagrams for D^+ decays. The D^+ decays ($c\bar{d} \to su\bar{d}\bar{d}$) have two $\bar{d}$ quarks in the final state and so decays such as $D^+ \to \bar{K}^0\pi^+$ can occur through both the external and internal spectator diagrams. There is no interference in D^0 or D_s^+ decays since the anti-quarks in the final state are not identical for D^0 decays ($c\bar{u} \to su\bar{d}\bar{u}$) and D_s^+ decays ($c\bar{s} \to su\bar{d}\bar{s}$).

However, the charm quark is still light enough that non-factorizable effects can have non-negligible contributions when compared with the simple spectator decays in many exclusive decays of D mesons. Two effects I will explore with the recent CLEO results are final state interactions (FSI) and W-exchange and W-annihilation decays.

---

[1] This work performed under the auspices of the US Department of Energy by the Lawrence Livermore National Laboratory under Contract W-7405ENG-48.

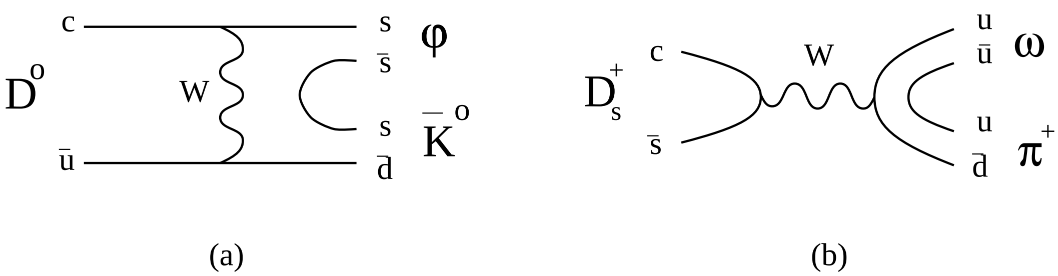

FIGURE 1. (a) W-exchange decay for $D^0 \to \phi\bar{K}^0$ and (b) W-annihilation decay for $D_s^+ \to \omega\pi^+$.

Final state interactions occur when the outgoing mesons get rescattered through intermediate resonances that lie near the D mass. For example, the exiting kaon and pion in the $D^0 \to K^-\pi^+$ decay can get rescattered through a highly excited $\bar{K}^0$ state and emerge as the final state $\bar{K}^0\pi^0$. This can enhance color-suppressed decays, since FSI feeds into these channels from the color-allowed decays. For the $D \to K\pi$ system, $\mathcal{B}(D^0 \to \bar{K}^0\pi^0)/\mathcal{B}(D^0 \to K^-\pi^+) = 0.62 \pm 0.13$, which is much larger than the naive expectation of 1/9 from color matching for quarks.

The above example is considered elastic FSI because the isospin and spin content of the initial and rescattered mesons do not change. On the other hand, inelastic FSI change the isospin and spin structure of the outgoing mesons. Some examples of inelastic FSI include $K\rho \leftrightarrow K^*\pi$, $KK \leftrightarrow \pi\pi$, and $K^*K^* \leftrightarrow KK$ rescattering.

W-exchange and W-annihilations diagrams for D decays such as $D^0 \to \phi\bar{K}^0$ and $D_s^+ \to \omega\pi^+$ are shown in Figure 1. These diagrams are helicity suppressed compared to the spectator diagrams, and the ratio of decay rates is $\Gamma_{annihilation}/\Gamma_{spectator} \sim M_q^2/M_D^2$, where M_q is the light quark mass. The only clear evidence of W-annihilation decays is in the purely leptonic D_s^+ decays [1]. The $D_s^+ \to \mu\nu$ decay has been observed by WA75, CLEO, BES, and most recently by E653 with a branching fraction of $\sim 0.5\%$. The L3 Collaboration [2] has recently observed $D_s^+ \to \tau\nu$ with a branching fraction of $(7.4 \pm 3.6)\%$.

CHARM PHYSICS WITH CLEO

The CLEO Collaboration consists of over 200 physicists from 24 universities. The data were selected from hadronic events collected by the CLEO II detector at the Cornell Electron Storage Ring (CESR). The CLEO II detector [3] is a large solenoidal detector with 67 tracking layers and a CsI electromagnetic calorimeter that provides efficient π^0 reconstruction. Charged kaon and pions are identified using specific ionization (dE/dx) and, when available, time-of-flight (TOF) information. The dE/dx and TOF information provide good

K/π separation up to 0.7 and 1.1 GeV/c, respectively. For high momentum particles the dE/dx relativistic rise provides greater than 2σ K/π separation, which is essential for separating rare B processes such as $B^0 \to \pi^+\pi^-$ from $B^0 \to K^+\pi^-$.

The data used in most of the analyses presented in this talk consist of an integrated luminosity of 4.8 fb^{-1} taken at and just below the $\Upsilon(4S)$ resonance, corresponding to $\sim 3 \times 10^6$ $B\bar{B}$ events and $\sim 5 \times 10^6$ $e^+e^- \to c\bar{c}$ events. In general, the charm physics analyses at CLEO use a common set of techniques to enhance the charmed hadron signal of interest. These include cuts on the D momentum, event shape, and D^* mass difference. The momentum spectrum for charmed hadrons from $e^+e^- \to c\bar{c}$ events is quite hard, so requiring the scaled D momentum to satisfy $x_p = p_D/\sqrt{E_{beam}^2 - M_D^2} > 0.5$ removes a lot of the combinatoric background from low momentum tracks. Charmed hadrons from B decays will have a momenta $x_p < 0.5$, and as a side-effect get eliminated. The event shape can be used to enhance charm events since $e^+e^- \to c\bar{c}$ events are jetty, whereas $B\bar{B}$ events decay isotropically because the B mesons are produced nearly at rest. Finally, the D^* mass trick is a powerful tool to enhance the D signal. The D^0, D^+, and D_s^+ mesons are required to come from $D^{*+} \to D^0\pi^+$, $D^{*+} \to D^+\pi^0$, and $D_s^{*+} \to D_s^+\gamma$ decays, respectively. The $D^* \to D\pi$ decay has limited phase space and the resolution of the mass difference, $\Delta M = M_{D\pi} - M_D$, is on average 10 times better than the invariant mass of the reconstructed D meson. So for example, a $D^{*+} \to D^0\pi^+$ tag reduces the D^0 signal by $4\times$ but reduces the background by $20 - 40\times$.

ISOSPIN ANALYSIS OF $D \to KK$

CLEO [4] has recently measured the branching fraction to the Cabibbo-allowed decay $D^+ \to K_s^0\pi^+$ and the Cabibbo-suppressed decay $D^+ \to K_s^0 K^+$. To extract the signals, we require a $D^{*+} \to D^+\pi^0$ tag and $x_p > 0.55$. We observe 70 ± 12 events for $D^+ \to K_s^0 K^+$ and 473 ± 26 events for $D^+ \to K_s^0\pi^+$ (shown in Figure 2.) The broad peak on the right of the $D^+ \to K_s^0 K^+$ signal are $D^+ \to K_s^0\pi^+$ events where the pion is mis-identified as a kaon, and the excess on the left is due to feed-down from $D \to K_s^0\pi\pi$ events.

The branching fractions are computed to be $\mathcal{B}(D^+ \to \bar{K}^0 K^+) = (0.70 \pm 0.12 \pm 0.07 \pm 0.05)\%$ and $\mathcal{B}(D^+ \to \bar{K}^0\pi^+) = (3.17 \pm 0.21 \pm 0.19 \pm 0.21 \pm 0.32)\%$, where the second error is systematic, the third is due to uncertainty in the normalization branching fraction, and the fourth error is due to possible interference from doubly Cabibbo suppressed decays (DCSD). The ratio of Cabibbo suppressed to allowed modes is 3.6σ higher than $\tan^2\theta_C \approx 0.05$. This is due to the destructive interference occurring in the $D^+ \to \bar{K}^0\pi^+$ decay mode.

Using CLEO's [1] previous results on $D^0 \to K^+K^-$, $K^0\bar{K}^0$, and $\bar{K}^0\pi^0$, we have measured the isospin amplitudes and relative phase shift for $D \to K\bar{K}$

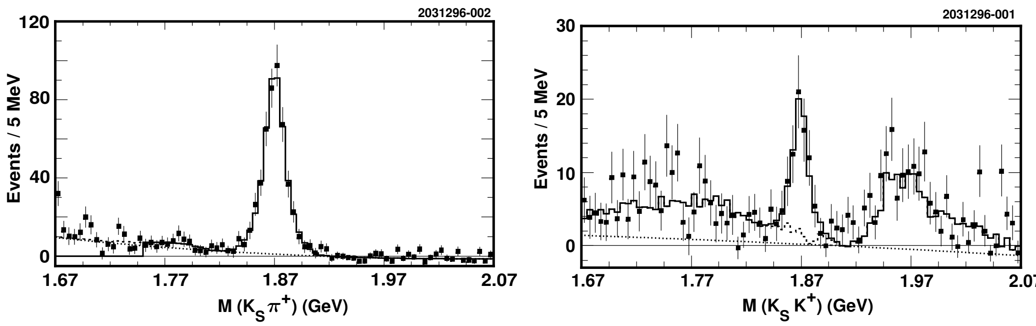

FIGURE 2. The invariant mass distribution for $K^0_s\pi^+$ and $K^0_s K^+$ combinations.

TABLE 1. Isospin analysis of $D \to KK$, $K\pi$, and $\pi\pi$.

Decay Mode	Amplitude Ratio	$\cos\delta$
$D \to KK$	$\left\|\frac{A_1}{A_0}\right\| = 0.61 \pm 0.11$	0.88 ± 0.09
$D \to K\pi$	$\left\|\frac{A_{3/2}}{A_{1/2}}\right\| = 0.27 \pm 0.03$	-0.12 ± 0.22
$D \to \pi\pi$	$\left\|\frac{A_2}{A_0}\right\| = 0.72 \pm 0.17$	0.14 ± 0.16

for the first time, and improved the isospin analysis for the $D \to K\pi$ system. The three decay modes $D^+ \to K^+K^-$, $D^+ \to K^0\bar{K}^0$, and $D^+ \to \bar{K}^0K^+$ can be described by two isospin amplitudes: A_0 and A_1, which correspond to the isospin 0 and 1 states for $K\bar{K}$. The decay rate amplitudes are linear combinations of the two isospin amplitudes.

$$\begin{aligned} Amp(D^+ \to K^+K^-) &= \sqrt{1/2}(A_1 + A_0) \\ Amp(D^+ \to K^0\bar{K}^0) &= \sqrt{1/2}(A_1 - A_0) \\ Amp(D^+ \to \bar{K}^0K^+) &= \sqrt{2}A_1 \end{aligned}$$

Similar isospin relations can be expressed for $D \to K\pi$ and $D \to \pi\pi$.

In the absence of FSI both A_0 and A_1 are real. When elastic FSI is turned on via resonant rescattering, the magnitude of the two isospin amplitudes do not change, but phase shifts can be introduced. This causes the K^+K^- and $K^0\bar{K}^0$ amplitudes to mix while the summed rate $\Gamma(D^+ \to K^+K^-)+\Gamma(D^+ \to K^0\bar{K}^0)$ stays unchanged. The $D^+ \to \bar{K}^0K^+$ amplitude remains invariant. Table 1 shows the isospin amplitude ratio and the relative phase shift (δ). The $\Delta I = 1/2$ rule in $K \to \pi\pi$ decays, which suppresses the $K^+ \to \pi^+\pi^0$ decay and implies $|A_2/A_0| \approx 0.05$, does not hold for $D \to \pi\pi$ decays which has a large A_2 amplitude. The striking difference in behavior is not well understood.

In the $D \to K\pi$ and $\pi\pi$ systems, the color suppressed modes are apprecia-

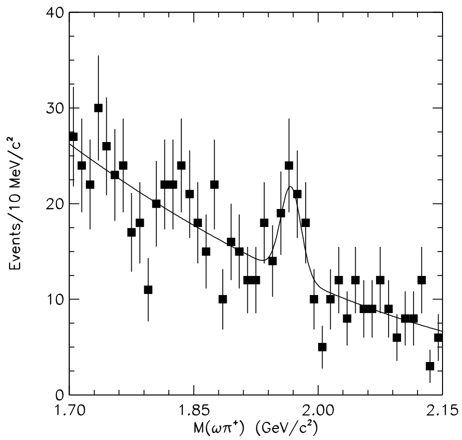

FIGURE 3. The invariant mass distribution for $\omega\pi^+$ combinations from tagged D_s^{*+} decays.

ble because $\delta \approx 90°$. The ratio of color suppressed to color allowed branching fractions are large: $\mathcal{B}(D^0 \to \bar{K}^0\pi^0)/\mathcal{B}(D^0 \to K^-\pi^+) = 0.62 \pm 0.13$ and $\mathcal{B}(D^0 \to \pi^0\pi^0)/\mathcal{B}(D^0 \to \pi^+\pi^-) = 0.63 \pm 0.18$. Turning off elastic FSI by setting $\delta \to 0$ would decrease the ratios significantly to 0.14 and 0.00, respectively.

On the other hand, the large ratio $\mathcal{B}(D^0 \to K^0\bar{K}^0)/\mathcal{B}(D^0 \to K^+K^-) = 0.12 \pm 0.03$ is unexpected. Because the $D^0 \to K^0\bar{K}^0$ decay can only occur at tree-level via W-exchange, assuming this rate is negligible we would expect $|A_1/A_0| = 1$ and the $D^0 \to K^0\bar{K}^0$ rate to be non-zero solely through FSI. But δ is consistent with being zero, so elastic FSI alone cannot be the explanation. Moreover, $|A_1/A_0|$ is 3.5σ from unity. So either W-exchange contributions are large or "inelastic" FSI, which can change both the magnitude and phase of A_0 and A_1, are appreciable.

OBSERVATION OF $D_S^+ \to \omega\pi^+$

D_s^+ decays into final states with no strangeness are strong candidates for W-annihilation decays, since D_s^+ spectator decays will always have an $\bar{s}$ quark in the final state. The $D_s^+ \to \omega\pi^+$ decay was expected to be a smoking gun for W-annihilation (see Figure 1) since the decay has no FSI contributions; the quantum numbers of the $\omega\pi^+$ system ($J^P = 0^-$ and $I^G = 1^+$) do not correspond to any known resonances. This is not true for $D_s^+ \to \pi\pi$ or $\rho\pi$ which are expected to have significant FSI.

However, this simple model is flawed. The $u\bar{d}$ quark pair from W-annihilation cannot hadronize into $\omega\pi^+$ due to G-parity conservation, which would require a second-class axial current. If, however, three gluons are connected to the initial state $c\bar{s}$ quark line, the modified W-annihilation process can occur with $W^+ \to u\bar{d} \to \pi^+$ and $ggg \to \omega$. Since the gluons also can carry spin, this process is no longer helicity suppressed. To further complicate the picture, although resonant FSI are not possible, Kamal *et al.* [5] and Buccella *et al.* [6] have suggested that non-resonant FSI can feed into $D_s^+ \to \omega\pi^+$ in the range $0.3 - 3\%$.

CLEO [7] has searched for the decay $D_s^+ \to \omega\pi^+$ with $\omega \to \pi^+\pi^-\pi^0$. Only $\omega \to \pi^+\pi^-\pi^0$ combinations in the central Dalitz region were selected, and $\omega\pi^+$ candidates were required to come from D_s^{*+} decays. We observed 36 ± 10 $D_s^+ \to \omega\pi^+$ events, shown in Figure 3. To verify there is no contribution from other $D_s^+ \to 4\pi$ decays, the ω mass cut was loosened and the 4π invariant mass was required to be in the D_s^+ signal region. A fit to the 3π invariant mass after a D_s^+ sideband subtraction yielded a comparable ω signal of 32 ± 12 events. The $\omega\pi^+$ combinations that failed the D_s^{*+} tag still contain an excess of 133 ± 57 events at the D_s^+ mass. The tagged and untagged results were combined and the branching fraction was normalized to the $D_s^+ \to \eta\pi^+$ decay to obtain $\mathcal{B}(D_s^+ \to \omega\pi^+)/\mathcal{B}(D_s^+ \to \eta\pi^+) = 0.16 \pm 0.04 \pm 0.03$. This is the first measurement of $D_s^+ \to \omega\pi^+$. The decay cannot occur from a simple spectator diagram, but must be due to FSI and/or W-annihilation.

MEASUREMENT OF $D_S^+ \to \eta\pi^+$, $\eta'\pi^+$, $\eta\rho^+$, AND $\eta'\rho^+$

The decays $D_s^+ \to \eta\pi^+$, $\eta'\pi^+$, $\eta\rho^+$, and $\eta'\rho^+$ comprise $25 - 30\%$ of the total D_s^+ branching fraction. An earlier CLEO analysis showed a 2σ departure from the factorization hypothesis that relates the two-body hadronic decay $D_s^+ \to \eta'\rho^+$ to the semileptonic decay $D_s^+ \to \eta'\ell\nu$:

$$\Gamma(D_s^+ \to \eta'\rho^+) = 6\pi^2 a_1^2 f_\rho^2 |V_{ud}|^2 \frac{d\Gamma}{dq^2}\,(D_s^+ \to \eta'\ell\nu)\Big|_{q^2=m_\rho^2}$$

CLEO measured $\Gamma(D_s^+ \to \eta'\rho^+)/\Gamma(D_s^+ \to \eta'\ell\nu) = 14.8 \pm 5.8$ and $\Gamma(D_s^+ \to \eta\rho^+)/\Gamma(D_s^+ \to \eta\ell\nu) = 4.3 \pm 1.1$, whereas theory predicts both ratios to be 2.9 [8].

With the full CLEO II dataset we have reexamined these branching fractions and the factorization hypothesis. For the $D_s^+ \to \eta\pi^+$ and $\eta'\pi^+$ modes, the η is reconstructed in the $\gamma\gamma$ and $\pi^+\pi^-\pi^0$ channels. To construct the $\eta\rho^+$ and $\eta'\rho^+$ invariant mass distributions, only the $\eta \to \gamma\gamma$ mode was used. Non-resonant $\eta^{(\prime)}\pi^+\pi^0$ contributions were reduced by requiring the $\pi^+\pi^0$ mass to be within 170 MeV/c^2 of the ρ^+ mass and the helicity angle to be $|\cos\theta_\pi| > 0.45$ since the ρ^+ must have zero helicity. There can still be non-negligible non-resonant feedthrough, so the $D_s^+ \to \eta\rho^+$ and $\eta'\rho^+$ branching fractions are extracted by relaxing the ρ cuts and fitting the Dalitz plot. Shown in Table 2 are the measured branching fractions along with the theoretical predictions. The variety of theoretical predictions assume form factors for the two-body decays from the pole model and from semileptonic decays. The predictions are consistent with the $\eta\pi^+$, $\eta'\pi^+$, and $\eta\rho^+$ branching fractions but cannot explain

TABLE 2. CLEO results and theoretical predictions for the $D_s^+ \to \eta\pi^+$, $\eta'\pi^+$, $\eta\rho^+$, and $\eta'\rho^+$ branching fractions.

D_s^+	$\Gamma/\Gamma(D_s^+ \to \phi\pi^+)$				
Mode	CLEO	VKK [9]	BSW [10]	BLP [6]	HK [11]
$\eta\pi^+$	$0.48 \pm 0.03 \pm 0.04$	0.9	1.0	0.3	0.6
$\eta'\pi^+$	$1.03 \pm 0.06 \pm 0.07$	0.8	0.6	1.3	1.6
$\eta\rho^+$	$2.98 \pm 0.20 \pm 0.39$	2.0	2.0	1.8	2.9
$\eta'\rho^+$	$2.78 \pm 0.28 \pm 0.30$	0.7	0.6	0.6	0.4

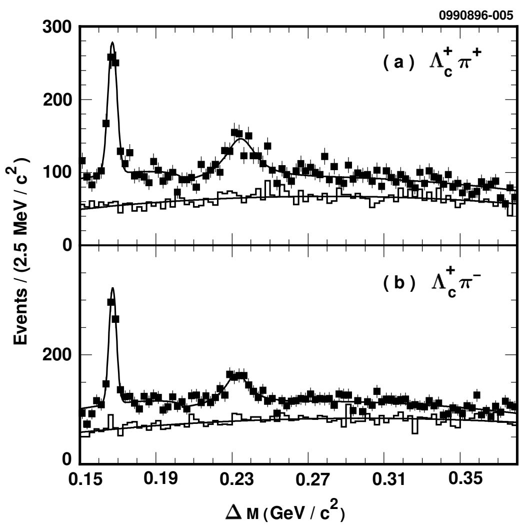

FIGURE 4. Mass difference spectra for (a) $\Lambda_c^+\pi^+$ candidates and (b) $\Lambda_c^+\pi^-$ candidates. The histogram shows the spectra for normalized sidebands of the Λ_c^+.

the large rate measured for $D_s^+ \to \eta'\rho^+$. Nor can FSI both resonant and non-resonant explain the discrepancy. In terms of the original factorization hypothesis, we now measure $\Gamma(D_s^+ \to \eta'\rho^+)/\Gamma(D_s^+ \to \eta'\ell\nu) = 12.0 \pm 4.3$ and $\Gamma(D_s^+ \to \eta\rho^+)/\Gamma(D_s^+ \to \eta\ell\nu) = 4.4 \pm 1.2$, compared with the theoretical prediction of 2.9. The uncertainty is primarily due to the uncertainty in the measured semileptonic decay rates. Ball *et al.* [12] has suggested that a modified W-annihilation diagram may be enhancing this mode, where two gluons connected to the initial $c\bar{s}$ quark line hadronize to the η'. This is analogous to the W-annihilation diagram for $D_s^+ \to \omega\pi^+$.

CHARMED BARYON SPECTROSCOPY

The family of charmed baryons is quite diverse. There is the isosinglet Λ_c^+ and the isotriplet Σ_c, the charmed-strange baryons Ξ_c and Ξ_c', and finally the

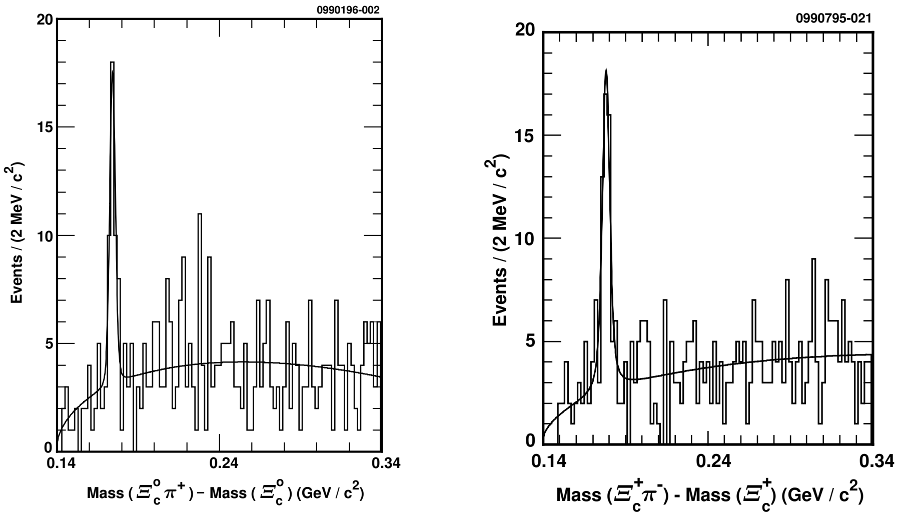

FIGURE 5. Mass difference spectra for (a) $\Xi_c^0\pi^+$ candidates and (b) $\Xi_c^+\pi^-$ candidates.

doubly-strange charmed baryon Ω_c. Most of the ground state charmed baryons with $J^P = \frac{1}{2}^+$ have been well measured. CLEO [13–15] has now observed many of the spin $\frac{3}{2}^+$ excitations of charmed baryons. These include the Σ_c^{*++} and Σ_c^{*0} which decay into $\Lambda_c^+\pi^+$ and $\Lambda_c^+\pi^-$, respectively; and the charmed-strange baryons Ξ_c^{*+} and Ξ_c^{*0} which are observed via the decay into $\Xi_c^0\pi^+$ and $\Xi_c^+\pi^-$, respectively. The Σ_c^{*++} and Σ_c^{*0} are part of an isospin triplet, but the Σ_c^{*+} has yet to be seen, primarily because of the difficulty of reconstructing its decay to $\Lambda_c^+\pi^0$.

The search for these spin excitations is similar to reconstructing D^* mesons. We accumulate large samples of the ground state charmed baryons, add a charged pion, apply an $x_p > 0.5$ cut, and examine the mass difference spectrum. For the Σ_c^{*++} and Σ_c^{*0} search, we start with ~ 15000 Λ_c^+ candidates from 13 decay modes. These include $\Lambda_c^+ \to pK^-\pi^+$ ($\sim$ 8400 evts), pK_s^0 ($\sim$ 1000 evts), $\Lambda\pi^+$ ($\sim$ 1100 evts), and $\Lambda\pi^+\pi^0$ ($\sim$ 900 evts). The $\Lambda_c^+\pi^+$ like-sign and $\Lambda_c^+\pi^-$ unlike-sign mass difference distributions are shown in Figure 4. Results of the fits to the Σ_c^* signals with a Breit-Wigner convoluted with the detector resolution are shown in Table 3. The broad peaks at $\Delta M \approx 233$ MeV/c^2 are the signals for Σ_c^{*++} and Σ_c^{*0}, in very good agreement with theoretical predictions. Both the $\Lambda_c^+\pi^+$ and $\Lambda_c^+\pi^-$ have nearly identical mass splittings, as is expected for isospin partners. The narrow peak at $\Delta M \approx 167$ MeV/c^2 is the ground state Σ_c. The Σ_c^* natural width is large because of the available phase space.

To search for the excited Ξ_c^{*+} and Ξ_c^{*0} baryons, we collect a large sample of the ground state Ξ_c^+ and Ξ_c^0 baryons. We use about 300 Ξ_c^+ candidates from the decays $\Xi_c^+ \to \Xi^-\pi^+\pi^+$, $\Xi^0\pi^+\pi^0$, and Σ^+K^{*0}; and about 300 Ξ_c^0 candidates from the decays $\Xi_c^0 \to \Xi^-\pi^+$, Ω^-K^+, $\Xi^-\pi^+\pi^0$, and $\Xi^0\pi^+\pi^-$. Combining

TABLE 3. Spin $\frac{3}{2}^+$ excited charmed baryons: Σ_c^* and Ξ_c^*.

Decay Mode	Signal (evts)	ΔM (MeV/c^2)	Γ (MeV/c^2)
$\Sigma_c^{*++} \to \Lambda_c^+\pi^+$	677^{+101}_{-93}	$234.5 \pm 1.1 \pm 0.8$	$17.9^{+3.8}_{-3.2} \pm 4.0$
$\Sigma_c^{*0} \to \Lambda_c^+\pi^-$	504^{+93}_{-83}	$232.6 \pm 1.0 \pm 0.8$	$13.0^{+3.7}_{-3.0} \pm 4.0$
$\Xi_c^{*+} \to \Xi_c^0\pi^+$	35 ± 9	$174.3 \pm 0.5 \pm 1.0$	< 3.9
$\Xi_c^{*0} \to \Xi_c^+\pi^-$	55 ± 12	$178.2 \pm 0.5 \pm 1.0$	< 5.5

the Ξ_c candidate with a charged pion and calculating the mass difference $\Delta M = M(\Xi_c\pi) - M(\Xi_c)$, we observe a narrow peak at $\Delta M = 174.3 \pm 0.5 \pm 1.0$ for $\Xi_c^0\pi^+$ and a narrow peak at $\Delta M = 178.2 \pm 0.5 \pm 1.0$ for $\Xi_c^+\pi^-$ combinations (see Figure 5 and Table 3). We identify these states as the Ξ_c^{*+} and Ξ_c^{*0}, respectively, because the theoretical mass predictions are consistent with our measurements and the two mass differences are nearly identical as is expected for isospin partners.

FUTURE PROSPECTS IN CHARM PHYSICS

In the Fall of 1995 the Silicon Vertex detector (SVX) was installed in the CLEO detector, and we have to date collected ~ 3 fb^{-1} of data, roughly 60% of the CLEO II dataset. The SVX is a three-layer, double-sided silicon strip detector that provides both $r\phi$ and z measurements. This will give a big boost to the charm physics program at CLEO. For the first time we will have decay length information for charmed hadrons. Vertex contrained fits to three-prong D^+ or two-prong D^0 decays will greatly reduce the combinatoric backgrounds. The $D^{*+} \to D^0\pi^+$ mass difference resolution has improved three-fold due to the SVX performance, Kalman track fitting, and vertex contrained fitting. Finally, the CLEO drift chamber is now using a helium-based gas in place of Argon-Ethane, which reduces the multiple scattering and reduces the Lorentz angle to provide improved hit efficiency over the entire drift cell.

Below is a wish list of future charm physics analyses that will benefit strongly from the SVX and improved tracking capabilities.

- Measure the D^0 and D^+ lifetimes with $1 - 2\%$ precision
- Untangle the DCSD and $D^0\bar{D}^0$ mixing contributions to $D^0 \to K^+\pi^-$ decays from the decay time information.
- Measure the natural width of D^{*+} to a precision of ~ 50 KeV
- Measure Cabibbo suppressed decays such as $D^+ \to \omega\ell^+\nu$
- Analyze $D^+ \to \bar{K}^{*0}\ell^+\nu$ form factors

The CLEO detector continues to evolve and will undergo a major upgrade in two years time when basically everything inside the CsI calorimeter will be replaced. The CESR peak luminosity is currently 4×10^{32} cm^{-2}s^{-1}; there is steady progress to increase the luminosity by a factor of 10. This will necessitate new rare earth and superconducting quadrupole magnets in the final focus. CLEO will build a new four-layer silicon detector and drift chamber which uses a helium-based gas. Finally, to identify pions and kaons with $> 4\sigma$ separation over the entire momentum and $\cos\theta$ range a ring imaging Cerenkov detector will be constructed.

In summary, the recent CLEO results in charm physics have explored final state interactions and W-annihilation processes in charmed meson decays. Isospin analyses of $D \to K\bar{K}$, $K\pi$, and $\pi\pi$ show significant FSI. The candidate W-annihilation decay $D_s^+ \to \omega\pi^+$ has been observed. The $D_s^+ \to \eta'\rho^+$ decay rate cannot be explained by factorization and may have a decay mechanism similar to that of $D_s^+ \to \omega\pi^+$. We have now observed many of the spin $\frac{3}{2}^+$ excited charmed baryons: Σ_c^{*++}, Σ_c^{*0}, Ξ_c^{*+}, and Ξ_c^{*0}. Discovery of the missing spectral states including the Ξ_c' and new orbitally excited charmed baryons are just around the corner. With luminosity and detector advancements, CLEO will continue to have a rich charm physics program in the years to come.

Acknowledgements: I would like to thank H. Yamamoto, J. Urheim, L. Gibbons, J. Bartelt, D. Kim, and M. Bishai for useful and stimulating discussions.

REFERENCES

1. Particle Data Group, R.M. Barnett *et al.*, Phys. Rev. D **54**, 1 (1996).
2. L3 Collaboration, preprint CERN-PPE/96-198.
3. Y. Kubota *et al.*, Nucl. Inst. and Meth. **A320**, 66 (1992).
4. M. Bishai *et al.*, Phys. Rev. Lett. **78**, 3261 (1997).
5. A.N. Kamal, N. Sinha, and R. Sinha, Phys. Rev. D **39**, 3503 (1989).
6. F. Buccella, M. Lusignoli, and A. Pugliese, Phys. Lett. B **379**, 249 (1996).
7. R. Balest *et al.*, preprint CLNS 97/1479, CLEO 97-8.
8. A.N. Kamal, Q.P. Xu, and A. Czarnecki, Phys. Rev. D **49**, 1330 (1994).
9. R.C. Verma, A.N. Kamal, and M.P. Khanna, Z. Phys. C **65**, 255 (1995).
10. M. Bauer, B. Stech, and M. Wirbel, Z. Phys. C **34**, 102 (1987).
11. I. Hinchliffe and T.A. Kaeding, Phys. Rev. D **54**, 914 (1996).
12. P. Ball, J.M. Frere, and M. Tytgat, Phys. Lett. B **365**, 367 (1996).
13. G. Brandenburg *et al.*, Phys. Rev. Lett. **78**, 2304 (1997).
14. L. Gibbons *et al.*, Phys. Rev. Lett. **77**, 810 (1996).
15. P. Avery *et al.*, Phys. Rev. Lett. **75**, 4364 (1995).